Eur. Phys. J. A (2019) **55**: 194
DOI 10.1140/epja/i2019-12922-0

THE EUROPEAN PHYSICAL JOURNAL A

Review

Hot-dense Lattice QCD*

USQCD Collaboration

Alexei Bazavov[1,a], Frithjof Karsch[2,3], Swagato Mukherjee[3,b], and Peter Petreczky[3]

[1] Department of Computational Mathematics, Science and Engineering and Department of Physics and Astronomy, Michigan State University, East Lansing, MI 48824, USA
[2] Fakultät für Physik, Universität Bielefeld, D-33615 Bielefeld, Germany
[3] Physics Department, Brookhaven National Laboratory, Upton, NY 11973, USA

Received: 19 August 2019 / Revised: 15 October 2019
Published online: 14 November 2019

Communicated by U.-G. Meißner

Abstract. This document is one of a series of white papers from the USQCD Collaboration. Here, we outline the opportunities for, prospects of and challenges to the Lattice QCD calculations relevant for the understanding of the phases and properties of hot-dense QCD matter. This program of Lattice QCD calculations is relevant to current and upcoming heavy-ion experimental programs at RHIC and LHC.

1 Executive summary

In 2018, the USQCD Collaboration's Executive Committee organized several subcommittees to recognize future opportunities and formulate possible goals for lattice field theory calculations in several physics areas. The conclusions of these studies, along with community input, are presented in seven white papers [1–6]. This white paper provides a roadmap for the current and future Lattice QCD calculations relevant for the understanding of the phases and properties of hot-dense QCD matter.

The matter that makes up the visible universe is mostly in the form of atomic nuclei. A nucleus is made up of protons and neutrons, which themselves were shown to be composed of more basic constituents called quarks, held together by the exchanges of gluons. The interactions of quarks and gluons are described by the theory of strong interactions, quantum chromodynamics (QCD). Under extreme conditions of high temperatures and/or densities hadrons cease to exist; quarks and gluons are liberated from the hadrons to form a new state of matter, known as the quark-gluon plasma (QGP). Understanding the phases of QCD and the properties of QGP is one of the key missions of the US nuclear physics program. An entire accelerator-based experimental facility, the Relativistic Heavy Ion Collider (RHIC) of Brookhaven National Laboratory, has been devoted to this mission. Many other experimental facilities across the world, including the Large Hadron Collider (LHC) at CERN, also have joined this pursuit. The understanding of phases and properties of hot-dense QCD matter from experimentation, as well as planning of future experiments, need many theoretical inputs. Lattice-regularized QCD, a technique suited for large-scale numerical calculations of QCD, is presently the only viable theoretical tool to study QCD in its full glory, by starting from the fundamental quark-gluon degrees of freedom and by taking into account the entire complexities of the strong interaction. In light of the ongoing and future heavy-ion experimental programs at RHIC and LHC, this USQCD white paper outlines the opportunities for, prospects of and challenges to the hot-dense Lattice QCD calculations in addressing the issues: i) phases and properties of baryon-rich QCD, ii) microscopy of QGP using heavy-quark probes, iii) nature of QCD phase transitions, iv) electromagnetic probes of QGP, v) jet energy loss in and viscosities of QGP.

2 Introduction

The mission of the US Department of Energy's (DOE) Nuclear Physics program is to discover, explore, and understand all forms of nuclear matter. As outlined in the 2015 NSAC Long Range Plan [7], a key component of the mission of this program is mapping the phase structures of quantum chromodynamics (QCD) and decoding the properties of quark-gluon plasma (QGP). DOE has dedicated an entire accelerator-based experimental program, the Relativistic Heavy-Ion Collider (RHIC) at Brookhaven

* Contribution to the Topical Issue "Opportunities for Lattice Gauge Theory in the Era of Exascale Computing" edited by William Detmold, Andreas Kronfeld, Ulf-G. Meißner.

[a] e-mail: bazavov@msu.edu (corresponding author)
[b] e-mail: swagato@bnl.gov

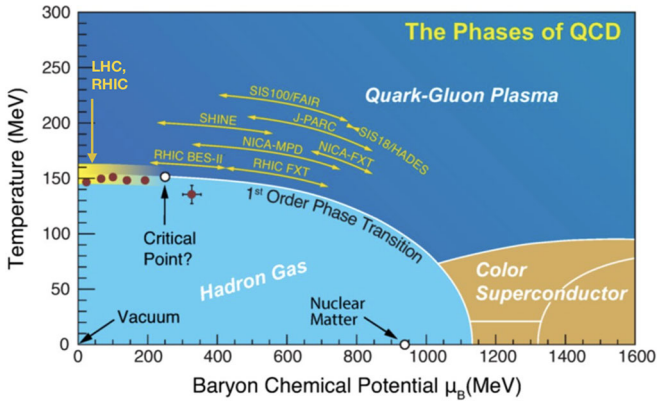

Fig. 1. A schematic phase diagram of QCD. Also, indicated are the ranges of explorations by various heavy-ion collision experiments.

National Laboratory (BNL), in pursuit of these causes. In the Large Hadron Collider (LHC) at CERN, Switzerland, the entire ALICE detector is devoted to exploration of properties and phases of QCD. Lattice-regularized QCD is, presently, the only viable technique that allows non-perturbative determinations of the properties and phase structures of hot-dense strong-interaction matter from its fundamental theory, QCD. Over the last decade, Lattice QCD has proven to be the most successful technique for model-independent, first-principle calculations of the phase structures and properties of hot-dense QCD matter; for recent reviews see refs. [8–10]. A schematic phase diagram of QCD is shown in fig. 1.

Experimental explorations at RHIC and LHC have revealed the surprising fact that the long-distance behavior of QGP closely resembles that of an almost inviscid fluid. QGP created at LHC and top RHIC energies consists of almost as much antimatter as matter, and is characterized by the nearly vanishing baryon-number chemical potential. Under these conditions the transition from the QGP to a hadron gas occurs through a smooth crossover, with many thermodynamic properties changing dramatically, but continuously, within a narrow range of temperature [11–13]. On the other hand, the baryon-rich QGP created at lower RHIC energies may experience a sharp first-order phase transition as it cools, with bubbles of QGP and bubbles of hadrons coexisting at a well-defined temperature. This region of co-existence ends in a critical point, where QGP and ordinary hadron-matter become indistinguishable.

The experimental explorations of phases of QCD and properties of QGP will continue over, and beyond, the next decade in many accelerator facilities across the world. For a recent comprehensive review on the science goals of the future heavy-ion collision experiments see ref. [14]. The two central scientific goals underlying these experiments are: i) Explorations of the phases of baryon-rich QCD, including the search for the QCD critical point; ii) Understanding the nature of QGP at shorter and shorter length scales. These themes also are at the heart of the planned upgrades of the US-based heavy-ion experiments at RHIC. The second phase of the RHIC Beam Energy Scan (BES-II) program [15], scheduled for 2019–21, will explore the QCD phase diagram. The sPHENIX experiment [16] at RHIC, with a planned start in 2023, will probe the short-distance physics of QGP using bottomonia and jets. Heavy flavor and jet physics also are key targets of the upgraded ALICE experiments starting 2021, as well as for the heavy-ion programs of the CMS, ATLAS and LHCb experiments at LHC. Another key component of the ALICE experiment will be establishing the nature of QCD transition at vanishing baryon density by looking at the higher moments of conserved charge fluctuations. Additionally, in future, various electromagnetic probes of QGP will be studied in detail both at RHIC and LHC. As in the past, success and planing of these future heavy-ion experimental programs crucially depend on various inputs from hot-dense Lattice QCD calculations. In this USQCD white paper we briefly outline the hot-dense Lattice QCD calculations that will not only enhance our fundamental understanding of the phases and properties of strong-interaction matter, but also significantly impact the heavy-ion collision experiments, particularly the ones at RHIC.

3 Phases and properties of baryon-rich QCD

Many properties of strong-interaction matter at non-zero temperature have been analyzed in hot-dense Lattice QCD calculations for vanishing values of chemical potentials (for recent reviews see, *e.g.*, [8, 10]). The pseudo-critical (crossover) temperature for the transition from a low temperature hadronic phase to a high temperature QGP phase has been examined and extrapolated to the continuum limit for physical values of two degenerate light (up, down) quark masses and a physical strange quark mass [12, 17]. A recent update of these calculations yields as pseudo-critical temperature $T_{pc} = (156 \pm 1.5)\,\mathrm{MeV}$ [18, 29], which is in excellent agreement with the freeze-out temperature for hadrons that has been extracted from particle yields measured by the ALICE Collaboration at LHC using a statistical hadronization model [31]. The phase boundary in the temperature and baryon chemical potential plane is shown in fig. 2. Also, continuum extrapolated results for the equation of state at vanishing baryon chemical potential, obtained with two different staggered fermion discretizations, agree quite well [19–21]. These results find applications in hydrodynamic modelings of the expanding matter created in heavy-ion collisions [22] and statistical analyses of freeze-out conditions.

The current focus of the lattice calculations of bulk properties of strong-interaction matter concerns the extension of these results to non-zero baryon chemical potential. As direct Lattice QCD simulations are not possible in this case, because of the notorious sign problem, calculations are done by either using Taylor expansions [23–25] or by analytical continuation of results obtained in simulations with imaginary chemical potentials [26–28]. Continuum-extrapolated results for the

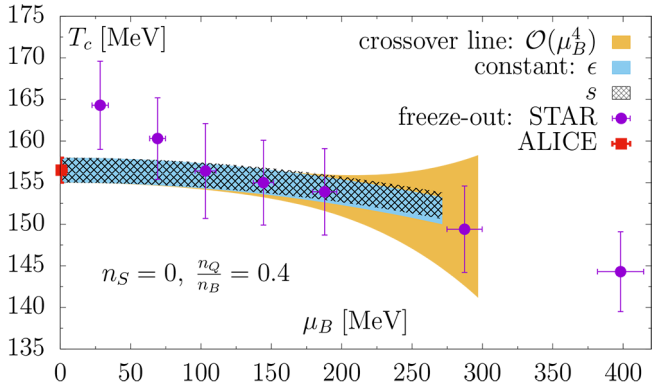

Fig. 2. Phase boundary for $(2+1)$-flavor QCD in the temperature and baryon chemical potential plane [29]. Also, shown are lines of constant energy and entropy density, as well as the freeze-out temperatures determined by STAR at RHIC [30] and ALICE at LHC [31].

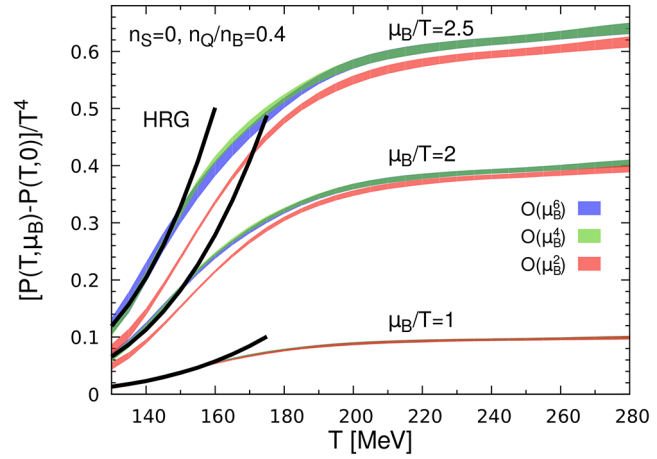

Fig. 3. The QCD pressure at non-zero baryon chemical potential for a strangeness neutral medium ($n_S = 0$) with net electric charge to baryon number density $n_Q/n_B = 0.4$ [25].

equation of state, now, have been obtained up to $\mathcal{O}(\mu_B^6)$ in a Taylor series, as well as through analytic continuations. This allows one to obtain results for bulk thermodynamic observables, such as the QCD equation of state [24,25], fig. 3, as well as the curvature of the pseudo-critical line [28,29] up to $\mu_B \simeq (1.5\text{–}2)T_{pc}$, which is sufficient as input for the analysis of data from the RHIC BES down to beam energies $\sqrt{s_{NN}} \simeq 12\,\text{GeV}$. *In order to provide input at lower beam energies that will be probed in the upcoming BES II higher precision for the existing expansion coefficients and results for higher order terms are needed.*

Good quantitative control over higher order Taylor expansion coefficients for bulk thermodynamic observables and fluctuations of conserved charges also is needed to estimate the convergence of these expansions [32]. For sufficiently high orders in the expansion the systematic of the sign changes in the expansion coefficients provide estimators for the possible location of a critical point in the $T - \mu_B$ phase diagram. Here the current estimates are limited by the statistical accuracy of the higher order expansion coefficients. Current estimates from up to 8th order expansion coefficients suggest that it is unlikely to find a critical point located at baryon chemical potentials smaller than $\mu_B \sim 2T_{pc}$ and temperatures larger than $T \sim 140\,\text{MeV}$. This is consistent with the even smaller value of the chiral phase transition temperature at vanishing light quark masses and physical value of the strange quark mass, which for vanishing baryon chemical potential is found to be $T_c^0 = 132^{+3}_{-6}$ [33]. *Improving over these estimates requires calculations at lower temperatures and higher accuracy on at least 10th order Taylor expansion coefficients.*

In the experimental searches for the QCD critical point measurements of higher order cumulants of net conserved charge fluctuations play an important role. The kurtosis and skewness of net proton-number (as a proxy for net baryon-number), net kaon number (as a proxy for net strangeness) and net electric charge fluctuations are being measured. Among these the kurtosis and skewness of net proton-number fluctuations show the strongest dependence on the beam energy and, hence, on μ_B. For $\sqrt{s_{NN}} \gtrsim 19\,\text{GeV}$ the systematic of kurtosis and skewness can be reproduced in Lattice QCD calculations of net baryon-number fluctuations. It could be shown that deviations from the simple Skellam distribution, as expected in hadron resonance gas (HRG) model calculations, i) are negative, ii) increase in magnitude with increasing μ_B, and iii) are about a factor three larger for the kurtosis than the skewness.

Similar calculations for strangeness and electric charge fluctuations do not yet exist, but need to be done. In particular, getting quantitative control over the net electric charge fluctuations is important as these can be compared directly to experimental results. The calculation of higher order cumulants of electric charge fluctuations in Lattice QCD is challenging for several reasons. They are dominated by contributions from pions. This introduces a large correlation length $\xi \sim 1/m_\pi$, and the results are very sensitive to finite volume effects. Moreover, continuum extrapolations are difficult as the pion sector is strongly distorted in Lattice QCD calculations with staggered fermions (because of taste symmetry violations), and calculations in other discretization schemes are much more demanding in terms of computational resources. Well-controlled results exist at present for the quadratic fluctuations (χ_2^Q) of net electric charges at $\mu_B = 0$, see fig. 4. *Calculations on large spatial lattices and closer to the continuum limit are needed to arrive at controlled continuum extrapolations for higher moments of net electric charge fluctuations.*

Although the HRG model provides a rather good description of many features found in Lattice QCD calculations below the crossover temperature, there are also many striking deviations from simple HRG model predictions. For instance, in the strangeness sector quadratic and quartic fluctuations are enhanced over those of simple HRG model predictions, which dominantly arise from larger baryon-number–strangeness correlations. This has been

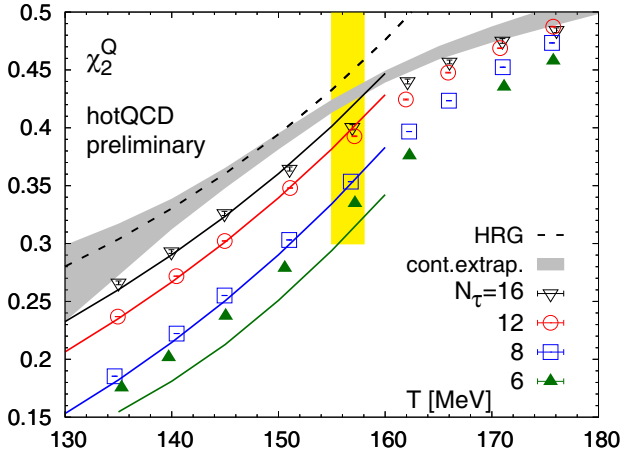

Fig. 4. Cut-off dependence of net electric charge fluctuations and continuum extrapolation (gray band). Lines show HRG model calculations taking into account modifications of the pion masses in calculations with staggered fermions (taste symmetry violations).

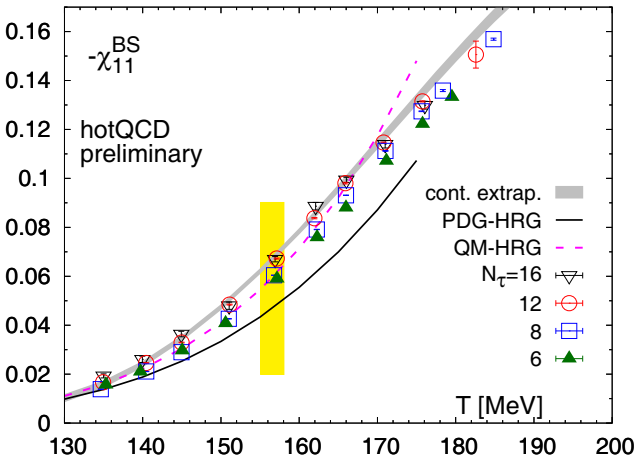

Fig. 5. Baryon-number–strangeness correlations at $\mu_B = 0$.

attributed to contributions from additional baryon resonances that are predicted to exist in quark model (QM-HRG) calculations, but have not yet been observed experimentally (PDG-HRG). They may be quite broad and their contribution may be taken care of in modified HRG models that take into account various decay channels of such unstable resonances through a virial expansion [34]. Lattice results for baryon-number–strangeness correlations χ_{11}^{BS} are shown in fig. 5 together with the PDG-HRG and QM-HRG model predictions. In order to better quantify deviations of Lattice QCD in various fluctuation and correlation observables from simple HRG model calculations, and control additional parameters that enter calculations with extended HRG models detailed analyses of higher order cumulants are needed. Correlations between fluctuations in different conserved charge sectors, *e.g.*, the correlation between baryon-number fluctuations and those of strangeness or electric charge, are currently being analyzed experimentally at RHIC and LHC. These correlations will also be studied in the BES-II at RHIC. *In order to calculate charge correlations at non-zero μ_B, again, accurate results on higher order cumulants are needed.*

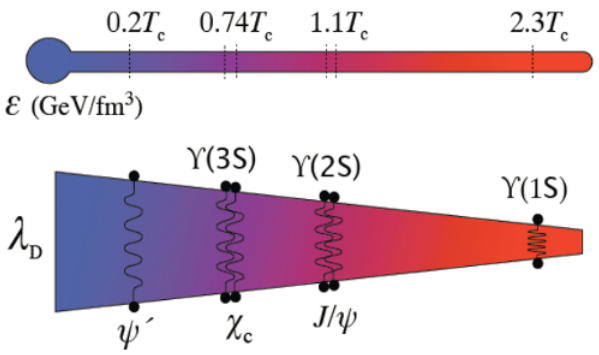

Fig. 6. Illustration of how sequential melting of quarkonia of different sizes, immersed in QGP, can probe QGP at different length and energy scales.

4 Probing QGP with heavy quarks

Hadrons containing heavy quarks provide an important probe of hot and dense matter created in heavy ion collisions. For example, quarkonia, mesons composed of a heavy quark and anti-quark have been proposed as the probe of the temperature of the produced medium [35]. A schematic illustration is shown in fig. 6. The presence of the hot deconfined medium weakens the binding effects between the heavy quarks, eventually leading to the dissolution of the quarkonia. The spectra and angular distributions of the hadrons with single heavy quark can be used to study the relaxation time scales of quark gluon plasma [36]. More precisely, these observables are sensitive to the heavy quark diffusion constant $D \sim M/Tt_{relax}$, with t_{relax} being the typical relaxation time scale of the medium and M being the heavy quark mass. Experimental results on the angular correlation and spectra of heavy flavor hadrons suggest that the relaxation time of heavy quarks is quite short indicating the strongly coupled nature of the matter created in heavy ion collisions, see ref. [37] for a recent review. Quarkonia and open heavy flavor hadrons are commonly referred to as the heavy flavor probes. There has been a large experimental effort at RHIC and LHC on the studies of heavy flavor probes. Future sPHENIX experiment at RHIC and ALICE upgrades largely target the physics of heavy flavor probes.

In-medium properties and/or dissolution of heavy flavor hadrons as well as the heavy quark diffusion constant are encoded in the spectral functions (see *e.g.* ref. [38] for a recent review). The properties of bound states are encoded in peak-like structures in the spectral functions at values of frequency ω of the order of the heavy quark mass. Heavy quark diffusion constant D is encoded in the behavior of the spectral function for $\omega \simeq 0$. In this region the spectral function has a peak, often called the transport peak. The width of the transport peak is proportional to

$T/(MD)$ [39] and, thus, is very small. At frequencies significantly above the bound state peaks the spectral function is featureless, and this part of the spectral function is referred to as the continuum. At sufficiently high temperatures the bound state peaks will broaden and disappear and the spectral function for ω larger than the quark mass will be described by the continuum, *i.e.* we will see the melting of the heavy quark bound states. It is expected that excited quarkonium states will "melt" at smaller temperatures than the more tightly bound ground state. This is often referred to as the sequential quarkonium melting.

While there is a direct relation between the spectral function and the Euclidean time correlation function appropriate reconstruction of the former is very challenging as the correlation function is available at a discrete set of points and has statistical errors (see discussion in ref. [38]). Moreover, the extent of the imaginary time direction is proportional to $1/T$, and, thus, becomes small at high temperature T. One can consider spatial correlation functions of meson operators, which are not restricted to small separation, but the relation between the correlation functions and spectral functions is less direct [40, 41]. Finally, we should point out that discretization effects due to the heavy quark mass could be also large, especially for the bottom quark.

The problems discussed above limited our ability to obtain reliable results on in-medium quarkonium properties. We could use the heavy quark mass to our advantage and combine Lattice QCD with an effective field theory (EFT) approach. Integrating out the heavy quark mass scale leads to an EFT called non-relativistic QCD (NRQCD), where the heavy quarks are represented by Pauli spinors and the creation of heavy quarks is encoded in higher dimensional operators [42]. Because the scale associated with the heavy quark mass has been integrated out there are no discretization errors associated with the heavy quark mass. The maximal Euclidean time extent in this formulation is $1/T$, which is twice larger than in the standard relativistic approach to heavy quarks. The high energy part of the spectral function is also smaller. As the result, the Euclidean correlation functions in this approach are more sensitive to the in-medium quarkonium properties. Lattice QCD studies of the quarkonium spectral functions in this approach have been reported using isotropic lattices, *i.e.*, lattices with the same lattice spacing in the temporal and spatial directions [43, 44], and also using anisotropic lattices, where the lattice spacing in time is smaller than the spatial lattice spacing [45–48]. The latter calculations did not reach the physical quark masses, while the former are limited to smaller lattices with temporal extents $N_\tau = 12$. Both calculations, however, show that $\Upsilon(1S)$ state can survive in the deconfined matter up to temperatures as high as 400 MeV, with only small medium modifications. The spectral functions reconstructed from $N_\tau = 12$ lattice calculations [44] are shown in fig. 7. One can clearly see the first peak corresponding to $\Upsilon(1S)$, with relatively little temperature dependence. Most of the studies of the quarkonium spectral functions, including the ones mentioned above rely on correlation functions of point meson operators, *i.e.* local quark bilinears. These correlators are dominated by the continuum part of the spectral function at high temperatures and thus have limited sensitivity to the in-medium quarkonium properties. This is especially true for the excited bottomonium states [44]. Using correlators of extended meson operators it is possible to get more sensitivity to the in-medium quarkonium properties as the relative contribution of the high frequency part of the spectral function will be smaller in this case. *In future it will be important to extend the calculations to physical quark masses using anisotropic lattices, so that quarkonium correlators with large number of data points in the time direction are available. Furthermore, correlation functions of extended meson operators should be studied in order to extract information about the in-medium properties of excited quarkonium states and confirm the expected pattern of sequential quarkonium melting. Also, one should consider lattice calculations on isotropic lattices much closer to the continuum limit* [49].

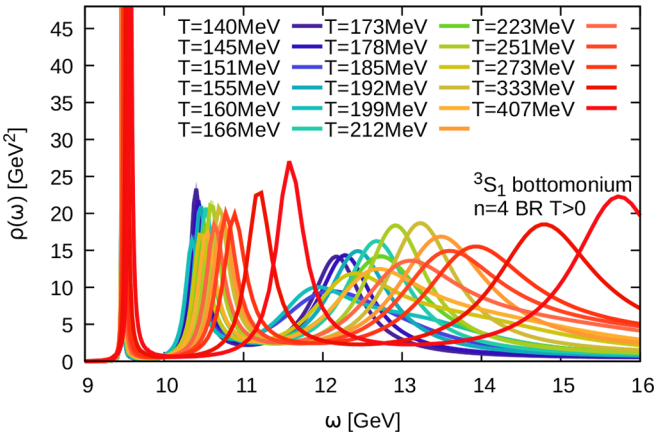

Fig. 7. The Υ spectral functions for different temperatures from lattice NRQCD calculations [44].

If we integrate out the energy scale associated with the inverse size of the quarkonium we get another EFT, the potential non-relativistic QCD (pNRQCD). The degrees of freedom in this EFT are the singlet and octet static meson fields, and the static quark anti-quark potential enters as the parameter in the Lagrangian of this EFT [50]. In this case, the static quark anti-quark potential entering the EFT Lagrangian not only becomes temperature dependent, but also turns out to be complex [51]. The complex potential can be calculated in weak coupling approach if the temperature is sufficiently high. When the binding energy is the smallest scale in the problem all higher energy scales can be integrated out and all the medium effects can be encoded in the temperature dependent potential [52]. Furthermore, the potential can be calculated on the lattice by considering temporal Wilson loops. Thus, the problem of the in-medium quarkonium properties is reduced to the calculation of Wilson loops at non-zero temperature and extracting the complex potential from them. The study of quarkonium properties in pNRQCD is very important as it provides a link between QCD and dynamical models of quarkonium production in

heavy ion collisions, see *e.g.* refs. [53, 54]. Lattice calculations of the complex potential have been carried out both in quenched [55] and $2+1$ flavor QCD [56, 57]. In the latter case the calculations were limited to temporal extent $N_\tau = 12$, and un-physically heavy dynamical light quark masses. *It will be important in the future to extend these calculations to physical quark masses and larger* N_τ.

As mentioned above the heavy quark diffusion coefficient is related to the behavior of the spectral functions at zero energy. The spectral function in this energy region has a peak, called the transport peak, which is a Lorentzian in the heavy quark limit, $\sigma_{trans}(\omega) = \chi_q \eta/(\omega^2 + \eta^2)$, χ_q being the heavy quark number susceptibility [39]. For heavy quarks $\eta = T/(MD) \ll 1$, *i.e.*, the transport peak is very narrow. Therefore, an accurate determination of its width and thus the diffusion constant D is extremely challenging [39]. However, we could take advantage of this feature and use the Heavy Quark Effective Theory (HEQT), where the heavy quark degrees of freedom are integrated out [58]. In this approach, one calculates the correlation function of chromo-electric field strength, which gives the momentum space diffusion coefficient κ as the $\omega \to 0$ limit of the corresponding spectral function. The spectral function in this case does not have a peak at $\omega \sim 0$ and is smoothly connected to the large ω region. Instead of determining the width of the transport peak one needs to determine the intercept at $\omega = 0$, which is much easier. Calculations along these lines have been performed in quenched QCD [59,60] and resulted in the value $\kappa = (1.8\text{–}3.4)T^3$. The reason for performing this calculation in quenched QCD is that the correlator of chromo-electric field strength is very noisy, and a novel multilevel algorithm is needed to obtain a good signal to noise ratio [61, 62]. This algorithm is presently only available for quenched QCD. *There are two possible ways to extend the existing calculations. One should consider higher temperatures, where weak coupling calculations are expected to work and comparisons between the lattice and weak coupling calculations are possible. This will be very important for validating the procedure of extracting the spectral functions from the lattice data. Second, one needs to develop algorithms in full QCD, which can deal with the noise problem. This remains a very challenging task despite recent progress* [63].

So far, we have discussed quarkonium in-medium properties. In-medium properties of open heavy flavor hadrons are far less explored on the lattice. Attempts to study D mesons at non-zero temperature have been presented in ref. [64]. An alternative way to study in-medium hadron properties is to consider spatial correlation functions [40, 41]. The spatial correlation functions are not limited to $1/T$ and, therefore, are more sensitive to the in-medium properties of hadrons. However, the relation of the spatial hadron correlation functions to the spectral functions is more complicated, involving a double integral transformation [40]. At low and very high temperatures the relation is simple and can be used to constrain the in-medium properties of heavy flavor hadrons.

Yet another way to obtain insights into the in-medium properties of open charm hadrons is to study charm fluctuations and correlations [65]. The corresponding lattice calculations indicate that charm hadronic excitations may exist above T_c [66]. Fluctuations of charm and charm-baryon correlations are also interesting from the point of view of providing information about the spectrum of charm hadrons in the vacuum. The lattice calculations indicate that there are additional charm baryons not listed by the Particle Data Group (PDG) but expected based on quark model calculations [65]. Current calculations have been performed on coarse lattices and/or unphysical quark masses. *It will be important to extend these calculations to finer lattices and physical quark masses.*

5 Nature of QCD phase transition

Although, by now, it is well-established that the transition from the low temperature hadronic phase of QCD to the asymptotically free quark-gluon phase is not a genuine phase transition, but a smooth crossover, it is expected that this crossover is sensitive to properties of strong-interaction physics that are described by a true phase transition in the limit of vanishing up and down quark masses, *i.e.*, in the chiral limit. Understanding the properties of strong-interaction physics at non-zero temperature and baryon chemical potential continues to be an extremely active field of research both experimentally and theoretically. It is, thus, of utmost importance to lay the ground for this research by firmly establishing the phase structure of QCD in the chiral limit. By doing so, we will be able to quantify to what extent the non-analytic features QCD that dominate the physics of strongly interacting matter in the chiral limit contribute to the non-perturbative properties of strongly interacting matter observed in nature.

A first obvious question that needs to be clarified is how the QCD transition temperature depends on the value of the light quark masses. What is the critical temperature in the chiral limit, and is this transition a 2nd order transition or does it turn into a 1st order transition at some critical value of the light quark masses? These questions are closely related to the question of (non-) existence of the QCD critical end-point in the $(T - \mu_B)$-plane. Unlike earlier studies of the nature of the transition in the chiral limit, that used unimproved staggered or Wilson fermion discretization schemes, current studies of the order of the chiral transition, performed with improved actions [33, 67, 68], do not find any hint for a first order transition down to Goldstone pion masses as small as 55 MeV. *These studies, currently, are performed on moderately sized lattices. Calculations closer to the chiral limit and proper continuum extrapolations are needed to confirm these results.*

First attempts to determine the chiral phase transition temperature in the continuum limit have been undertaken recently. Our current understanding is that the chiral phase transition in QCD with two mass-less quarks and a physical strange quark occurs at $T_c = 132^{+3}_{-6}$ MeV [33], *i.e.*, at a temperature about 25 MeV smaller than the QCD transition temperature [18]. The chiral susceptibility from which T_c has been extracted [33] is shown in fig. 8.

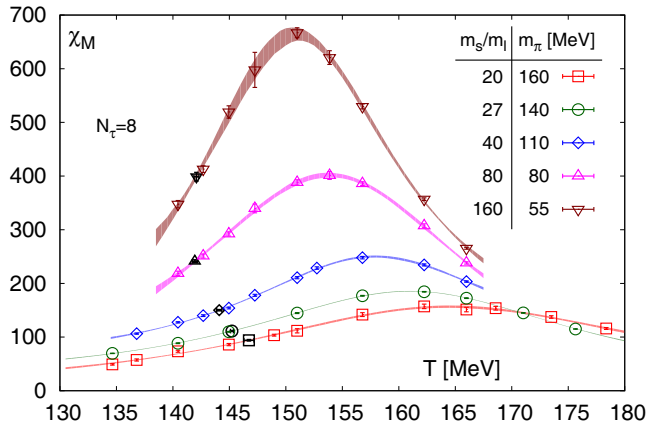

Fig. 8. The chiral susceptibility of $(2+1)$-flavor QCD on lattices with temporal extents $N_\tau = 8$ and for various values of the light quark masses [33].

The nature of the chiral phase transition also crucially depends on the fate of the axial $U_A(1)$ symmetry at high temperatures. This was understood early on by Pisarski and Wilczek [69]. If the $U_A(1)$ symmetry gets restored close to the chiral phase transition the nature of the phase transition can change since the $O(4)$ symmetry is no longer relevant. In fact, for long time it has been thought that the chiral phase transition would be first order, if the $U_A(1)$ symmetry is effectively restored at T_c since no universality class corresponding to a larger symmetry group was known. However, recently it has been shown that a universality class for $O(2)\times O(N)$ models in three dimensions exists [70,71]. This makes it possible that the QCD phase transition is second order, and at the same time, may lead to an effective restoration of the axial $U_A(1)$ symmetry. Irrespective of the order of the phase transition, the effective restoration of $U_A(1)$ symmetry at T_c may imply that the above analysis based on the $O(4)$ scaling may not be valid, and an additional pseudo-Goldstone excitation, like a light η' meson, may appear in the transition region. It has been suggested that a light η' meson can be seen experimentally [72–74] though more work is needed to verify this assertion.

A crucial indicator for the chiral $U_A(1)$ symmetry restoration is the structure of the low-lying eigenvalue spectrum of the Dirac operator. In order for $U_A(1)$ to remain broken a non-zero density of near-zero modes needs to be present on finite lattices, which eventually will give rise to a non-zero density of zero modes that can be responsible for $U_A(1)$ symmetry breaking. In recent calculations within chiral fermion discretization schemes and physical values of the light quark masses arguments have been put forward in favor of $U_A(1)$ symmetry restoration close to the flavor symmetry restoring transition [75]. However, these calculations still are done on rather small lattices, which makes it difficult to eliminate the influence of finite-volume effects on the relevant small Dirac eigenvalues. Moreover, due to the large difference between the crossover temperature at physical values of the quark masses and the chiral phase transition temperature it is obvious that these calculations, at present, only allow to conclude that $U_A(1)$ symmetry breaking effects become small at temperatures $T \geq 1.2T_c$. *More detailed studies close to the chiral limit and on large lattices are needed to arrive at definitive conclusions on the role of* $U_A(1)$ *symmetry breaking close to the chiral phase transition.*

6 Electromagnetic probes of QGP

QGP is a thermal medium consisting of electrically charged quarks and, hence, naturally emits photons. Due to the smallness of the electromagnetic coupling and limited extent of the medium created during collisions of heavy ions, photons emitted inside QGP escape the medium without subsequent interactions. Also, QGP-emitted virtual photons decay into lepton pairs (dileptons) and escape the medium without further interaction. Thus, photons and di-leptons provide valuable information regarding properties of hot-dense QCD matter [76], and are experimentally sought after observables at RHIC and LHC [77]. Furthermore, the strengths of the experimental signals of the chiral magnetic effect sensitively depend on how long the magnetic field, produced at very early times, lasts inside expanding QGP [78]; the lifetime of the magnetic field trapped inside QGP is entirely governed by the value of the electrical conductivity of QGP [79].

Lattice QCD calculations of di-lepton rates, photon emissivity and electrical conductivity rely upon reliable extraction of the spectral function from Euclidean correlation function of the vector current. These studies demand very precise calculations of the vector current two-point correlation function on lattices having very large temporal extents. Present Lattice QCD results are either based on quenched approximation [80,81], or carried out on small lattices with un-physically heavy dynamical quarks [82,83]. *To have an impact on the experiments, in future, Lattice QCD calculations of electromagnetic probes of QGP need to be carried out on large lattices with physical dynamical quarks.*

7 Exploring jet energy loss and viscosities

Probing properties of QGP through detailed studies of jet quenching, *i.e.*, the energy loss of a fast moving parton inside QGP, is one of the key components of the future sPHENIX experiment at RHIC, as well as the LHC heavy-ion program. Jet quenching in QGP is characterized in terms of a quantity called $\hat{q}$ that measures the momentum transfer squared per unit time. A fully non-perturbative estimate of $\hat{q}$ is highly desired. As the mechanism of jet quenching involves dynamics of a fast moving parton on the light cone, a direct Lattice QCD-based determination of $\hat{q}$ is an extremely challenging problem. However, at temperatures significantly higher than the QCD crossover temperature one can use an EFT-based approach to address this problem [84, 85]. In this case,

one can use the 3-dimensional EFT, the electrostatic QCD (EQCD), to calculate $\hat{q}$ by separating the perturbative and non-perturbative parts of the calculation. One can solve EQCD on the lattice and determine the non-perturbative part of $\hat{q}$. Calculations along these lines have been presented in ref. [86]. A different approach to calculate the jet quenching parameter $\hat{q}$ based on the field strength correlator on the light cone, was suggested in refs. [87,88]. In lattice setup this reduces to the calculations of the expectation value of a local operator. It is not clear, however, to what extent local operators in Euclidean space time can approximate the physics on the light cone.

The calculations of the shear and bulk viscosities in Lattice QCD are also extremely challenging. There are at least two reasons for this. First, the viscosities are defined in terms of correlators of energy-momentum stress tensor, which involves gluonic quantities. Gluonic quantities are very noisy when evaluated on the lattice. Second, the correlators of energy-momentum stress tensor are dominated by the high frequency modes, and the corresponding spectral functions are proportional to ω^4 at large frequencies. As the result, the corresponding correlators have little sensitivity to the transport peak. Viscosities that are different by an order of magnitude will lead to changes in the correlation functions by less than a 1% [89]. To deal with the first problem multi-level algorithm should be used [61,62]. This, presently, limits the calculations to pure $SU(3)$ gauge theory. To deal with the second problem on can use Ward identities to obtain correlators that correspond to spectral functions behaving like ω^2 at large frequencies [90,91]. Using these tricks and anisotropic lattices the best determination for shear viscosity to entropy ratio gives $\eta/s = 0.17(2)$ for pure $SU(3)$ gauge theory at $T = 1.5T_c$ [89]. This seems to confirm the strongly coupled nature of QGP, though the systematic uncertainties due to modeling the spectral functions may not be fully understood. Another study finds $\eta/s = 0.27(7)$ for $1.5T_c$ [92], which is higher than the above estimate. Thus, a better understanding of the analytic form of the spectral function is needed. Analytic calculations on the weak coupling side may help in this respect [93].

Given the extremely challenging nature of both these problems, presently, it is unclear whether fully-controlled lattice calculations, with light dynamical fermions, of $\hat{q}$ and QGP viscosities can be achieved in the near future. However, albeit their challenges, these problems present immense opportunities for hot-dense Lattice QCD to impact the explorations of QGP properties. Thus, it will be very important to explore all possible new avenues, both algorithmic and formalism wise, to make significant progress in addressing these issues on the lattice.

8 Computational challenges

In the last decade, significant progresses toward quantifying the features of the hot and dense strong-interaction matter have been made in the *ab initio* Lattice QCD calculations, as has been outlined in the previous sections. It became possible with the continued DOE support for computing hardware, as well as software development efforts. Currently members of USQCD utilize the dedicated USQCD hardware funded by DOE and the large-scale computational resources available through the INCITE and ALCC programs.

However, many challenges still remain, which require significant algorithmic developments and computational power to address them. The need for software development for future architectures has been recognized by DOE through the continuation of funding of the Nuclear Physics SciDAC-4, as well as the Exascale Computing Program. Based on the existing software, available expertise, ongoing software development efforts and the projected computational resources that are going to be available, we outline below the computational challenges in relation to the hot-dense Lattice QCD physics program.

At present, there is no direct method to carry out Monte Carlo simulations of QCD at $\mu_B > 0$ due to the sign problem. The way to proceed is to expand the pressure in μ_B/T and calculate the physical observables as Taylor expansions in this quantity. In practice, this requires calculating operators of high order, which are noisy and require very large statistics. The traces of operators are estimated stochastically and, thus, one repeatedly solves the Dirac equation on the same gauge field configuration with many, order thousands, different sources. This problem requires high-capacity computing, since the work can be split among many GPUs or multi-core nodes, requiring communication only among few of them. To control the approach to the continuum limit one also needs to perform calculations at finer lattices, *i.e.*, with larger temporal and spatial dimensions.

While for calculations at $\mu_B > 0$ the main computational cost is in the number of measurements per given gauge field configuration, studying the properties of QCD close to the chiral limit poses a different challenge. The cost of inverting the Dirac operator is inversely proportional to the square of the lightest quark mass. Given that the current simulations place the bound on the first-order region of the Columbia plot[1] at the pion mass around 55 MeV or smaller, one needs to perform simulations at light quark masses, significantly lower than their physical values. On top of that, to maintain full control over the finite-volume effects, one needs larger lattice volumes than in simulations with the physical light quark masses. For the large lattices the problem is in the high-capability domain, where efficient inter-node parallelism is needed. The ongoing software development efforts are towards multi-GPU codes as well as a hybrid MPI-OpenMP model that can make efficient use of multi-core architectures. Besides that, algorithmic improvements such as multigrid [95–97] are needed. At present, efficient multigrid algorithm has been designed for Wilson fermions, while it remains an open question if the same level of efficiency can be achieved for staggered fermions [97].

[1] A two-dimensional diagram that represents the expected order of the finite-temperature transition in QCD as a function of the light and strange quark masses, as first appeared in ref. [94].

Simulations at fine lattices and low quark masses suffer from critical slowing down, related to the freezing of the gauge field topology. This area may need further algorithmic improvements, since subtle properties such as the restoration of the anomalous $U_A(1)$ symmetry depend on the proper sampling of the topology of the gauge fields. The symmetry properties of lattice fermions may also be important in this problem. While Domain Wall Fermions (DWF) are not used in large-scale hot-dense QCD calculations due to their high computational cost, they possess almost exact chiral symmetry on the lattice. To fully understand the phenomena associated with the $U_A(1)$ symmetry above the chiral crossover temperature a program of large-scale DWF calculations might be needed in future.

The fate of the heavy-quark bound states in Quark-Gluon Plasma has been of considerable interest since the Matsui-Satz conjecture [35], that suppression of J/ψ yields due to the screening effects in the thermal medium may provide an unambiguous signal of QGP formation. In reality, there are several competing effects and the overall picture turned out to be more complicated. To fully address the properties of heavy quarkonia one needs theoretical understanding of the medium modification of their spectral functions that encode full information about the states. Since Lattice QCD is formulated in the Euclidean space-time formalism, the real-time properties, such as the spectral functions, are hard to access. In practice, one computes Euclidean correlation functions, from which the spectral functions can be reconstructed by solving and inverse problem. This inverse problem is very ill-posed since the available input information is limited by the number of lattice points in the temporal direction.

The isotropic (*i.e.* the same lattice spacing in the temporal and spatial directions) gauge field configurations that will be generated to address the QCD at $\mu_B > 0$ and close to the chiral limit are limited to the temporal extent of $N_\tau = 24$ and maybe $N_\tau = 32$ in the longer term. For robust spectral function reconstruction one needs lattices with N_τ of order a hundred. Thus, a dedicated program of computations on anisotropic lattices is needed. With anisotropy factor of 6 one can reach finite-temperature lattices $32^3 \times 48$ to $64^3 \times 96$ that correspond to temperatures of 2–3T_c.

Apart from generating dedicated finite-temperature lattices with large N_τ, designing new reconstruction algorithms is also of importance. The Bayesian techniques such as the Maximum Entropy Method (MEM) [98] are often used. Recently a modification of MEM has been introduced in [99], which however still has some deficiencies, such as ringing, that may produce false peaks in the spectral functions. Further improvements, perhaps based on the recent progress in the field of machine learning, may be helpful in this area.

From the methodological point of view, the problem of heavy quarks in QGP is deeply related to first-principle calculations of transport properties of QGP. Calculation of shear and bulk viscosities, photon emissivity, electrical conductivity, and all such tranport properties depend on fully-controlled reliable extraction of spectral functions from the corresponding Euclidean correlation functions. The viscosities represent the grand challenge since they come from the noisiest and the least understood channel, related to the correlators of the energy-momentum stress tensor. Thus, developing the inverse problem methodology for heavy quarks and electromagnetic probes will pave the way for first-principle shear and bulk viscosity calculations. In the long run, the latter will require development of new methods beyond what is currently available on the lattice. Possible collaboration with data scientists, that deal with various facets of the inverse problem spanning across many scientific domains, may prove useful for the lattice community. At the same time, continued focused efforts on algorithmic improvements to produce anisotropic lattices with large temporal extents will ensure near-term availability of high-quality next-generation data sets of gauge field samples.

Steady progress of Lattice QCD calculations in general and at finite temperature and density in particular in the last several decades has been achieved by constant improvement of the theoretical understanding of the underlying quantum field theory as well as development of new efficient algorithms for simulating the theory on the lattice. Oftentimes, this happens by trial and error and it is thus hard to predict which particular direction may lead to a breakthrough. It is thus important apart from maintaining the well-established and planned-ahead research program to leave some room for trying new ideas. Our discussion will be incomplete without mentioning some high-risk high-return directions, which, if progress is achieved, will significantly impact the class of problems that can be addressed in hot-dense Lattice QCD.

The long-standing sign problem is still drawing attention in the lattice community. One possible angle to attack the problem is to develop a formalism that allows for simulating arbitrary, including complex, actions. This is being pursued with the complex Langevin and the Lefshetz thimble methods. Selected recent work can be found in [100–103]. Another angle is to rely on the Taylor expansion and/or the imaginary chemical potential methods, but to find ways to speed them up dramatically, so that much higher orders in the expansion become achievable [104, 105]. In the inverse problem class that spans from in-medium properties of heavy-flavor states to transport properties of QGP an interesting possibility is an attempt to perform simulations in the real-time Schwinger-Keldysh formalism [106–108].

Data Availability Statement This manuscript has no associated data or the data will not be deposited. [Authors' comment: This study is a review of results existing in the literature. Thus, no new data were generated.]

References

1. USQCD Collaboration (R. Brower, A. Hasenfratz, E.T. Neil *et al.*), https://doi.org/10.1140/epja/i2019-12901-5 (2019).
2. USQCD Collaboration (V. Cirigliano, Z. Davoudi *et al.*), https://doi.org/10.1140/epja/i2019-12889-8 (2019).
3. USQCD Collaboration (W. Detmold, R.G. Edwards *et al.*), https://doi.org/10.1140/epja/i2019-12902-4 (2019).
4. USQCD Collaboration (B. Joó, C. Jung *et al.*), https://doi.org/10.1140/epja/i2019-12919-7 (2019).
5. USQCD Collaboration (A.S. Kronfeld, D.G. Richards *et al.*), https://doi.org/10.1140/epja/i2019-12916-x (2019).
6. USQCD Collaboration (C. Lehner, S. Meinel *et al.*), https://doi.org/10.1140/epja/i2019-12891-2 (2019).
7. Nuclear Science Advisory Committee (A. Aprahamian *et al.*), *Reaching for the Horizon: The 2015 Long Range Plan for Nuclear Science* (2015) http://inspirehep.net/record/1398831/files/2015_LRPNS_091815.pdf.
8. H.T. Ding, F. Karsch, S. Mukherjee, Int. J. Mod. Phys. E **24**, 1530007 (2015) arXiv:1504.05274.
9. R.A. Soltz, C. DeTar, F. Karsch, S. Mukherjee, P. Vranas, Annu. Rev. Nucl. Part. Sci. **65**, 379 (2015) arXiv:1502.02296.
10. C. Ratti, Rep. Prog. Phys. **81**, 084301 (2018) arXiv:1804.07810.
11. T. Bhattacharya *et al.*, Phys. Rev. Lett. **113**, 082001 (2014) arXiv:1402.5175.
12. A. Bazavov *et al.*, Phys. Rev. D **85**, 054503 (2012) arXiv:1111.1710.
13. Y. Aoki, G. Endrodi, Z. Fodor, S.D. Katz, K.K. Szabo, Nature **443**, 675 (2006) arXiv:hep-lat/0611014.
14. W. Busza, K. Rajagopal, W. van der Schee, Annu. Rev. Nucl. Part. Sci. **68**, 339 (2018) arXiv:1802.04801.
15. D. Keane, J. Phys. Conf. Ser. **878**, 012015 (2017).
16. PHENIX Collaboration (A. Adare *et al.*), arXiv:1501.06197 (2015).
17. Y. Aoki, S. Borsanyi, S. Durr, Z. Fodor, S.D. Katz, S. Krieg, K.K. Szabo, JHEP **06**, 088 (2009) arXiv:0903.4155.
18. HotQCD Collaboration (P. Steinbrecher), Nucl. Phys. A **982**, 847 (2019) arXiv:1807.05607.
19. S. Borsanyi, Z. Fodor, C. Hoelbling, S.D. Katz, S. Krieg, K.K. Szabo, Phys. Lett. B **730**, 99 (2014) arXiv:1309.5258.
20. HotQCD Collaboration (A. Bazavov *et al.*), Phys. Rev. D **90**, 094503 (2014) arXiv:1407.6387.
21. A. Bazavov, P. Petreczky, J.H. Weber, Phys. Rev. D **97**, 014510 (2018) arXiv:1710.05024.
22. J. Auvinen, K.J. Eskola, P. Huovinen, H. Niemi, R. Paatelainen, P. Petreczky, PoS **Confinement2018**, 135 (2018) arXiv:1811.01792.
23. R.V. Gavai, S. Gupta, Phys. Rev. D **68**, 034506 (2003) arXiv:hep-lat/0303013.
24. S. Borsányi, G. Endrodi, Z. Fodor, S.D. Katz, S. Krieg, C. Ratti, K.K. Szabó, JHEP **08**, 053 (2012) arXiv:1204.6710.
25. A. Bazavov *et al.*, Phys. Rev. D **95**, 054504 (2017) arXiv:1701.04325.
26. M. D'Elia, M.P. Lombardo, Phys. Rev. D **67**, 014505 (2003) arXiv:hep-lat/0209146.
27. J.N. Guenther, R. Bellwied, S. Borsányi, Z. Fodor, S.D. Katz, A. Pasztor, C. Ratti, K.K. Szabó, Nucl. Phys. A **967**, 720 (2017) arXiv:1607.02493.
28. C. Bonati, M. D'Elia, F. Negro, F. Sanfilippo, K. Zambello, Phys. Rev. D **98**, 054510 (2018) arXiv:1805.02960.
29. HotQCD Collaboration (A. Bazavov *et al.*), Phys. Lett. B **795**, 15 (2019) arXiv:1812.08235.
30. STAR Collaboration (L. Adamczyk *et al.*), Phys. Rev. C **96**, 044904 (2017) arXiv:1701.07065.
31. A. Andronic, P. Braun-Munzinger, K. Redlich, J. Stachel, Nature **561**, 321 (2018) arXiv:1710.09425.
32. S. Borsanyi, Z. Fodor, J.N. Guenther, S.K. Katz, K.K. Szabó, A. Pasztor, I. Portillo, C. Ratti, arXiv:1805.04445 (2018).
33. H.T. Ding *et al.*, Phys. Rev. Lett. **123**, 062002 (2019) arXiv:1903.04801.
34. C. Fernández-Ramírez, P.M. Lo, P. Petreczky, Phys. Rev. C **98**, 044910 (2018) arXiv:1806.02177.
35. T. Matsui, H. Satz, Phys. Lett. B **178**, 416 (1986).
36. G.D. Moore, D. Teaney, Phys. Rev. C **71**, 064904 (2005) arXiv:hep-ph/0412346.
37. A. Beraudo *et al.*, Nucl. Phys. A **979**, 21 (2018) arXiv:1803.03824.
38. A. Mocsy, P. Petreczky, M. Strickland, Int. J. Mod. Phys. A **28**, 1340012 (2013) arXiv:1302.2180.
39. P. Petreczky, D. Teaney, Phys. Rev. D **73**, 014508 (2006) arXiv:hep-ph/0507318.
40. F. Karsch, E. Laermann, S. Mukherjee, P. Petreczky, Phys. Rev. D **85**, 114501 (2012) arXiv:1203.3770.
41. A. Bazavov, F. Karsch, Y. Maezawa, S. Mukherjee, P. Petreczky, Phys. Rev. D **91**, 054503 (2015) arXiv:1411.3018.
42. W.E. Caswell, G.P. Lepage, Phys. Lett. B **167**, 437 (1986).
43. S. Kim, P. Petreczky, A. Rothkopf, Phys. Rev. D **91**, 054511 (2015) arXiv:1409.3630.
44. S. Kim, P. Petreczky, A. Rothkopf, JHEP **11**, 088 (2018) arXiv:1808.08781.
45. G. Aarts, C. Allton, T. Harris, S. Kim, M.P. Lombardo, S.M. Ryan, J.I. Skullerud, JHEP **07**, 097 (2014) arXiv:1402.6210.
46. G. Aarts, C. Allton, S. Kim, M.P. Lombardo, S.M. Ryan, J.I. Skullerud, JHEP **12**, 064 (2013) arXiv:1310.5467.
47. G. Aarts, C. Allton, S. Kim, M.P. Lombardo, M.B. Oktay, S.M. Ryan, D.K. Sinclair, J.I. Skullerud, JHEP **03**, 084 (2013) arXiv:1210.2903.
48. G. Aarts, C. Allton, S. Kim, M.P. Lombardo, M.B. Oktay, S.M. Ryan, D.K. Sinclair, J.I. Skullerud, JHEP **11**, 103 (2011) arXiv:1109.4496.
49. Y. Burnier, H.T. Ding, O. Kaczmarek, A.L. Kruse, M. Laine, H. Ohno, H. Sandmeyer, JHEP **11**, 206 (2017) arXiv:1709.07612.
50. N. Brambilla, A. Pineda, J. Soto, A. Vairo, Nucl. Phys. B **566**, 275 (2000) arXiv:hep-ph/9907240.
51. N. Brambilla, J. Ghiglieri, A. Vairo, P. Petreczky, Phys. Rev. D **78**, 014017 (2008) arXiv:0804.0993.
52. P. Petreczky, C. Miao, A. Mocsy, Nucl. Phys. A **855**, 125 (2011) arXiv:1012.4433.
53. N. Brambilla, M.A. Escobedo, J. Soto, A. Vairo, Phys. Rev. D **97**, 074009 (2018) arXiv:1711.04515.
54. N. Brambilla, M.A. Escobedo, J. Soto, A. Vairo, Phys. Rev. D **96**, 034021 (2017) arXiv:1612.07248.
55. A. Rothkopf, T. Hatsuda, S. Sasaki, Phys. Rev. Lett. **108**, 162001 (2012) arXiv:1108.1579.

56. Y. Burnier, O. Kaczmarek, A. Rothkopf, Phys. Rev. Lett. **114**, 082001 (2015) arXiv:1410.2546.
57. A. Bazavov, Y. Burnier, P. Petreczky, Nucl. Phys. A **932**, 117 (2014) arXiv:1404.4267.
58. S. Caron-Huot, M. Laine, G.D. Moore, JHEP **04**, 053 (2009) arXiv:0901.1195.
59. D. Banerjee, S. Datta, R. Gavai, P. Majumdar, Phys. Rev. D **85**, 014510 (2012) arXiv:1109.5738.
60. A. Francis, O. Kaczmarek, M. Laine, T. Neuhaus, H. Ohno, Phys. Rev. D **92**, 116003 (2015) arXiv:1508.04543.
61. M. Luscher, P. Weisz, JHEP **09**, 010 (2001) arXiv:hep-lat/0108014.
62. H.B. Meyer, JHEP **01**, 048 (2003) arXiv:hep-lat/0209145.
63. M. Ce, L. Giusti, S. Schaefer, Phys. Rev. D **93**, 094507 (2016) arXiv:1601.04587.
64. A. Kelly, A. Rothkopf, J.I. Skullerud, Phys. Rev. D **97**, 114509 (2018) arXiv:1802.00667.
65. A. Bazavov *et al.*, Phys. Lett. B **737**, 210 (2014) arXiv:1404.4043.
66. S. Mukherjee, P. Petreczky, S. Sharma, Phys. Rev. D **93**, 014502 (2016) arXiv:1509.08887.
67. A. Bazavov, H.T. Ding, P. Hegde, F. Karsch, E. Laermann, S. Mukherjee, P. Petreczky, C. Schmidt, Phys. Rev. D **95**, 074505 (2017) arXiv:1701.03548.
68. H.T. Ding, P. Hegde, F. Karsch, A. Lahiri, S.T. Li, S. Mukherjee, P. Petreczky, Nucl. Phys. A **982**, 211 (2019) arXiv:1807.05727.
69. R.D. Pisarski, F. Wilczek, Phys. Rev. D **29**, 338 (1984).
70. P. Calabrese, P. Parruccini, A. Pelissetto, E. Vicari, Phys. Rev. B **70**, 174439 (2004) arXiv:cond-mat/0405667.
71. A. Pelissetto, E. Vicari, Phys. Rev. D **88**, 105018 (2013) arXiv:1309.5446.
72. T. Csorgo, R. Vertesi, J. Sziklai, Phys. Rev. Lett. **105**, 182301 (2010) arXiv:0912.5526.
73. R. Vertesi, T. Csorgo, J. Sziklai, Phys. Rev. C **83**, 054903 (2011) arXiv:0912.0258.
74. M. Vargyas, T. Csö, R. Vertesi, Cent. Eur. J. Phys. **11**, 553 (2013) arXiv:1211.1166.
75. JLQCD Collaboration (K. Suzuki, S. Aoki, Y. Aoki, G. Cossu, H. Fukaya, S. Hashimoto), EPJ Web of Conferences **175**, 07025 (2018) arXiv:1711.09239.
76. R. Rapp, H. van Hees, Eur. Phys. J. A **52**, 257 (2016) arXiv:1608.05279.
77. S. Campbell, Nucl. Phys. A **967**, 177 (2017) arXiv:1704.06307.
78. D.E. Kharzeev, J. Liao, S.A. Voloshin, G. Wang, Prog. Part. Nucl. Phys. **88**, 1 (2016) arXiv:1511.04050.
79. L. McLerran, V. Skokov, Nucl. Phys. A **929**, 184 (2014) arXiv:1305.0774.
80. H.T. Ding, O. Kaczmarek, F. Meyer, Phys. Rev. D **94**, 034504 (2016) arXiv:1604.06712.
81. J. Ghiglieri, O. Kaczmarek, M. Laine, F. Meyer, Phys. Rev. D **94**, 016005 (2016) arXiv:1604.07544.
82. G. Aarts, C. Allton, A. Amato, P. Giudice, S. Hands, J.I. Skullerud, JHEP **02**, 186 (2015) arXiv:1412.6411.
83. B.B. Brandt, A. Francis, T. Harris, H.B. Meyer, A. Steinberg, EPJ Web of Conferences **175**, 07044 (2018) arXiv:1710.07050.
84. S. Caron-Huot, Phys. Rev. D **79**, 065039 (2009) arXiv:0811.1603.
85. M. Benzke, N. Brambilla, M.A. Escobedo, A. Vairo, JHEP **02**, 129 (2013) arXiv:1208.4253.
86. M. Panero, K. Rummukainen, A. Schäfer, Phys. Rev. Lett. **112**, 162001 (2014) arXiv:1307.5850.
87. A. Kumar, A. Majumder, C. Nonaka, PoS **LATTICE2018**, 169 (2018) arXiv:1811.01329.
88. A. Majumder, Phys. Rev. C **87**, 034905 (2013) arXiv:1202.5295.
89. S. Borsanyi, Z. Fodor, M. Giordano, S.D. Katz, A. Pasztor, C. Ratti, A. Schaefer, K.K. Szabo, B.C. Toth, Phys. Rev. D **98**, 014512 (2018) arXiv:1802.07718.
90. H.B. Meyer, JHEP **08**, 031 (2008) arXiv:0806.3914.
91. H.B. Meyer, Eur. Phys. J. A **47**, 86 (2011) arXiv:1104.3708.
92. N. Astrakhantsev, V. Braguta, A. Kotov, JHEP **04**, 101 (2017) arXiv:1701.02266.
93. J. Hong, D. Teaney, Phys. Rev. C **82**, 044908 (2010) arXiv:1003.0699.
94. F.R. Brown, F.P. Butler, H. Chen, N.H. Christ, Z.h. Dong, W. Schaffer, L.I. Unger, A. Vaccarino, Phys. Rev. Lett. **65**, 2491 (1990).
95. J. Brannick, R.C. Brower, M.A. Clark, J.C. Osborn, C. Rebbi, Phys. Rev. Lett. **100**, 041601 (2008) arXiv:0707.4018.
96. R. Babich, J. Brannick, R.C. Brower, M.A. Clark, T.A. Manteuffel, S.F. McCormick, J.C. Osborn, C. Rebbi, Phys. Rev. Lett. **105**, 201602 (2010) arXiv:1005.3043.
97. R.C. Brower, M.A. Clark, A. Strelchenko, E. Weinberg, Phys. Rev. D **97**, 114513 (2018) arXiv:1801.07823.
98. M. Asakawa, T. Hatsuda, Y. Nakahara, Prog. Part. Nucl. Phys. **46**, 459 (2001) arXiv:hep-lat/0011040.
99. Y. Burnier, A. Rothkopf, Phys. Rev. Lett. **111**, 182003 (2013) arXiv:1307.6106.
100. G. Aarts, E. Seiler, D. Sexty, I.O. Stamatescu, PoS **LATTICE2016**, 036 (2016) arXiv:1611.02930.
101. G. Aarts, E. Seiler, D. Sexty, I.O. Stamatescu, PoS **LATTICE2016**, 092 (2016) arXiv:1611.02931.
102. A. Alexandru, G. Basar, P.F. Bedaque, H. Lamm, S. Lawrence, Phys. Rev. D **98**, 034506 (2018) arXiv:1807.02027.
103. S. Bluecher, J.M. Pawlowski, M. Scherzer, M. Schlosser, I.O. Stamatescu, S. Syrkowski, F.P.G. Ziegler, SciPost Phys. **5**, 044 (2018) arXiv:1803.08418.
104. P. de Forcrand, B. Jäger, EPJ Web of Conferences **175**, 14022 (2018) arXiv:1710.07305.
105. P. de Forcrand, B. Jäger, PoS **LATTICE2018**, 178 (2018) arXiv:1812.00869.
106. J. Pawlowski, A. Rothkopf, Phys. Lett. B **778**, 221 (2018) arXiv:1610.09531.
107. A. Alexandru, G. Basar, P.F. Bedaque, S. Vartak, N.C. Warrington, Phys. Rev. Lett. **117**, 081602 (2016) arXiv:1605.08040.
108. A. Alexandru, G. Basar, P.F. Bedaque, G.W. Ridgway, Phys. Rev. D **95**, 114501 (2017) arXiv:1704.06404.